

Measurement of the branching ratio of the decay $K_L \rightarrow \pi^\pm e^\mp \nu$ and extraction of the CKM parameter $|V_{us}|$

NA48 Collaboration

A. Lai, D. Marras

Dipartimento di Fisica dell'Università e Sezione dell'INFN di Cagliari, I-09100 Cagliari, Italy

A. Bevan, R.S. Dosanjh², T.J. Gershon³, B. Hay, G.E. Kalmus, C. Lazzeroni,
D.J. Munday, E. Olaiya⁴, M.A. Parker, T.O. White, S.A. Wotton

Cavendish Laboratory, University of Cambridge, Cambridge, CB3 0HE, UK¹

G. Barr⁵, G. Bocquet, A. Ceccucci, T. Cuhadar-Dönszelmann⁶, D. Cundy⁷,
G. D'Agostini, N. Doble⁸, V. Falaleev, L. Gatignon, A. Gonidec, B. Gorini, G. Govi,
P. Grafström, W. Kubischta, A. Lacourt, A. Norton, S. Palestini, B. Panzer-Steindel,
H. Taureg, M. Velasco⁹, H. Wahl¹⁰

CERN, CH-1211 Genève 23, Switzerland

C. Cheshkov¹¹, A. Gaponenko, P. Hristov¹¹, V. Kekelidze, L. Litov, D. Madigojine,
N. Molokanova, Yu. Potrebenikov, S. Stoynev, G. Tatishvili¹², A. Tkatchev,
A. Zinchenko

Joint Institute for Nuclear Research, Dubna 141980, Russian Federation

I. Knowles, V. Martin⁹, R. Sacco¹³, A. Walker

Department of Physics and Astronomy, University of Edinburgh, JCMB King's Buildings, Mayfield Road, Edinburgh, EH9 3JZ, UK

M. Contalbrigo, P. Dalpiaz, J. Duclos, P.L. Frabetti¹⁴, A. Gianoli, M. Martini,
F. Petrucci, M. Savrié

Dipartimento di Fisica dell'Università e Sezione dell'INFN di Ferrara, I-44100 Ferrara, Italy

A. Bizzeti¹⁵, M. Calvetti, G. Collazuol⁸, G. Graziani¹⁶, E. Iacopini, M. Lenti,
F. Martelli¹⁷, M. Veltri¹⁷

Dipartimento di Fisica dell'Università e Sezione dell'INFN di Firenze, I-50125 Firenze, Italy

H.G. Becker, K. Eppard, M. Eppard¹¹, H. Fox⁹, A. Kalter, K. Kleinknecht, U. Koch,
L. Köpke, P. Lopes da Silva, P. Marouelli, I. Pellmann¹⁹, A. Peters¹¹, B. Renk,
S.A. Schmidt, V. Schönharting, Y. Schué, R. Wanke, A. Winhart, M. Wittgen²⁰

Institut für Physik, Universität Mainz, D-55099 Mainz, Germany¹⁸

J.C. Chollet, L. Fayard, L. Iconomidou-Fayard, J. Ocariz, G. Unal, I. Wingerter-Seez

Laboratoire de l'Accélérateur Linéaire, IN2P3-CNRS, Université de Paris-Sud, 91898 Orsay, France²¹

G. Anzivino, P. Cenci, E. Imbergamo, P. Lubrano, A. Mestvirishvili, A. Nappi,
M. Pepe, M. Piccini

Dipartimento di Fisica dell'Università e Sezione dell'INFN di Perugia, I-06100 Perugia, Italy

R. Casali, C. Cerri, M. Cirilli¹¹, F. Costantini, R. Fantechi, L. Fiorini, S. Giudici,
G. Lamanna, I. Mannelli, G. Pierazzini, M. Sozzi

Dipartimento di Fisica, Scuola Normale Superiore e Sezione dell'INFN di Pisa, I-56100 Pisa, Italy

J.B. Cheze, J. Cogan, M. De Beer, P. Debu, A. Formica, R. Granier de Cassagnac²²,
E. Mazzucato, B. Peyaud, R. Turlay, B. Vallage

DSM/DAPNIA–CEA Saclay, F-91191 Gif-sur-Yvette, France

M. Holder, A. Maier¹¹, M. Ziolkowski

Fachbereich Physik, Universität Siegen, D-57068 Siegen, Germany²³

R. Arcidiacono, C. Biino, N. Cartiglia, R. Guida, F. Marchetto, E. Menichetti,
N. Pastrone

Dipartimento di Fisica Sperimentale dell'Università e Sezione dell'INFN di Torino, I-10125 Torino, Italy

J. Nassalski, E. Rondio, M. Szleper⁹, W. Wislicki, S. Wronka

Soltan Institute for Nuclear Studies, Laboratory for High Energy Physics, PL-00-681 Warsaw, Poland²⁴

H. Dibon, G. Fischer, M. Jeitler, M. Markytan, I. Mikulec, G. Neuhofer, M. Pernicka,
A. Taurok, L. Widhalm

Österreichische Akademie der Wissenschaften, Institut für Hochenergiephysik, A-1050 Wien, Austria²⁵

Received 25 August 2004; accepted 27 September 2004

Available online 7 October 2004

Editor: W.-D. Schlatter

Abstract

We present a new measurement of the branching ratio R of the decay $K_L \rightarrow \pi^\pm e^\mp \nu$, denoted as K_{e3} , relative to all charged K_L decays with two tracks, based on data taken with the NA48 detector at the CERN SPS. We measure $R = 0.4978 \pm 0.0035$. From this we derive the K_{e3} branching fraction and the weak coupling parameter $|V_{us}|$ in the CKM matrix. We obtain $|V_{us}|f_+(0) = 0.2146 \pm 0.0016$, where $f_+(0)$ is the vector form factor in the K_{e3} decay.

© 2004 Published by Elsevier B.V.

¹ Funded by the UK Particle Physics and Astronomy Research Council.

² Present address: Ottawa-Carleton Institute for Physics, Carleton University, Ottawa, Ontario K1S 5B6, Canada.

³ Present address: High Energy Accelerator Research Organization (KEK), Tsukuba, Japan.

⁴ Present address: Rutherford Appleton Laboratory, Chilton, Didcot, Oxon, OX11 0QX, UK.

⁵ Present address: Department of Physics, University of Oxford, Denis Wilkinson Building, Keble Road, Oxford, UK, OX1 3RH.

⁶ Present address: University of British Columbia, Vancouver, BC, Canada, V6T 1Z1.

⁷ Present address: Istituto di Cosmogeofisica del CNR di Torino, I-10133 Torino, Italy.

⁸ Present address: Scuola Normale Superiore e Sezione dell'INFN di Pisa, I-56100 Pisa, Italy.

⁹ Present address: Northwestern University, Department of Physics and Astronomy, Evanston, IL 60208, USA.

¹⁰ Present address: Dipartimento di Fisica dell'Università e Sezione dell'INFN di Ferrara, I-44100 Ferrara, Italy.

¹¹ Present address: PH Department, CERN, CH-1211 Geneva 23, Switzerland.

¹² Present address: Carnegie Mellon University, Pittsburgh, PA 15213, USA.

¹³ Present address: Department of Physics, Queen Mary, University of London, Mile End Road, London, E1 4NS.

¹⁴ Present address: Joint Institute for Nuclear Research, Dubna 141980, Russian Federation.

¹⁵ Dipartimento di Fisica dell'Università di Modena e Reggio Emilia, I-41100 Modena, Italy.

¹⁶ Present address: DSM/DAPNIA–CEA Saclay, F-91191 Gif-sur-Yvette, France.

¹⁷ Istituto di Fisica dell'Università di Urbino, I-61029 Urbino, Italy.

¹⁸ Funded by the German Federal Minister for Research and Technology (BMBF) under contract 7MZ18P(4)-TP2.

¹⁹ Present address: DESY Hamburg, D-22607 Hamburg, Germany.

²⁰ Present address: SLAG, Stanford, CA 94025, USA.

²¹ Funded by Institut National de Physique des Particules et de Physique Nucléaire (IN2P3), France.

²² Present address: Laboratoire Leprince-Ringuet, École polytechnique (IN2P3), Palaiseau, 91128 France.

²³ Funded by the German Federal Minister for Research and Technology (BMBF) under contract 056SI74.

²⁴ Supported by the KBN under contract SPUB-M/CERN/P03/DZ210/2000 and using computing resources of the Interdisciplinary Center for Mathematical and Computational Modelling of the University of Warsaw.

²⁵ Funded by the Federal Ministry of Science and Transportation under the contract GZ 616.360/2-IV GZ 616.363/2-VIII, and by the Austrian Science Foundation under contract P08929-PHY.

1. Introduction

The unitary condition for the first row of the CKM quark mixing matrix is at present fulfilled only at the 10% C.L. [1]. This has renewed interest in the measurement of the coupling constant V_{us} for strangeness-changing weak transitions. The most precise information on V_{us} comes from the decay $K_L \rightarrow \pi^\pm e^\mp \nu$, which is a vector transition, and therefore is protected from SU(3) breaking effects by the Ademollo–Gatto theorem [2]. We present here a new measurement with improved experimental precision.

2. Apparatus

The experiment was performed using the NA48 detector in a beam of long-lived neutral kaons produced at the 450 GeV proton synchrotron SPS at CERN. The neutral K_L beam was derived at an angle of 2.4 mrad from an extracted proton beam hitting a beryllium target. The decay region starts at the exit face of the last of three collimators 126 m downstream of the target. The experiment was originally designed and used for the precision measurement of direct CP violation in kaon decays [3]. We report here on a study of semileptonic decays, for which data were taken in a pure K_L beam in September 1999. The main elements of the detector relevant for this exposure are the following.

The magnetic spectrometer consists of four drift chambers (DCH), each with 8 planes of sense wires oriented along four projections, each one rotated by 45 degrees with respect to the previous one. The spatial resolution achieved per projection is 100 μm , and the time resolution for an event is 0.7 ns. The volume between the chambers is filled with helium near atmospheric pressure. The spectrometer magnet is a dipole with a field integral of 0.883 T m and is placed after the first two chambers. The distance between the first and the last chamber is 21.8 meters. The spectrometer is designed to measure the momenta of the charged particles with high precision—the momentum resolution is given by

$$\frac{\sigma(p)}{p} = 0.48\% \oplus 0.009p\%, \quad (1)$$

where p is in GeV/c.

The hodoscope is placed downstream from the last drift chamber. It consists of two planes of scintillators segmented in horizontal and vertical strips and arranged in four quadrants. The signals are used for a fast coincidence of two charged particles in the trigger. The time resolution from the hodoscope is ≈ 200 ps per track.

The electromagnetic calorimeter (Lkr) is a quasi-homogeneous calorimeter based on liquid krypton, with tower readout. The 13212 readout cells have cross sections of $\approx 2 \times 2 \text{ cm}^2$. The electrodes extend from the front to the back of the detector in a small angle accordion geometry. The Lkr calorimeter measures the e^\mp and γ energies by summing the ionization from their electromagnetic showers. The energy resolution is:

$$\frac{\sigma(E)}{E} = \frac{3.2\%}{\sqrt{E}} \oplus \frac{9.0\%}{E} \oplus 0.42\%, \quad (2)$$

where E is in GeV.

Charged decays were triggered with a two-level trigger system. The trigger requirements were two charged particles in the scintillator hodoscope or in the drift chambers coming from a vertex in the decay region.

A more detailed description of the NA48 setup can be found elsewhere [3].

3. Data analysis

3.1. Analysis strategy and events selection

The basic quantity measured in this experiment is the ratio R of decay rates of K_{e3} decays relative to all decays with two charged particles in the final state, mainly $\pi e \nu$, $\pi \mu \nu$ (called $K_{\mu 3}$), $\pi^+ \pi^- \pi^0$ (called $K_{3\pi}$), $\pi^+ \pi^-$ (called $K_{2\pi}$) and $3\pi^0$ with Dalitz decay of one π^0 , denoted as $\pi^0 \pi^0 e e \gamma$ or $\pi^0 \pi^0 \pi_D^0$. Since the neutral decay modes to $3\pi^0$, $2\pi^0$ and $\gamma\gamma$ have been measured, and the correction for events with four tracks $B(4T)$ is small, the sum of branching ratios of all K_L decay modes with two charged tracks $B(2T)$ is experimentally known [1]

$$B(2T) = 1 - \frac{\Gamma(K_L \rightarrow \text{all neutral})}{\Gamma(K_L \rightarrow \text{all})} - B(4T)$$

$$\begin{aligned}
&= 1 - B(3\pi^0) - B(2\pi^0) - B(\gamma\gamma) \\
&\quad + B(\pi^0\pi^0\pi_D^0) - B(4T) \\
&= 1.0048 - B(3\pi^0). \tag{3}
\end{aligned}$$

Since contributions from K_S meson or Λ hyperon decays and from rare K_L decays are negligible, less than 2×10^{-5} , we obtain the K_{e3} branching ratio using $B(2T)$:

$$\begin{aligned}
B(e3) &= \frac{\Gamma(K_{e3})}{\Gamma(K_L \rightarrow \text{all})} \\
&= \frac{\Gamma(K_{e3})}{\Gamma(K_L \rightarrow \text{all 2-track})} B(2T). \tag{4}
\end{aligned}$$

In this experiment, we therefore measure the ratio of K_{e3} events to all 2-track events N_{2T} divided by their acceptances a_e or a_{2T} , respectively:

$$R = \frac{N_e/a_e}{N_{2T}/a_{2T}}. \tag{5}$$

Both numbers, N_e and N_{2T} are extracted from the same sample of about 80 million recorded 2-track events. These were reconstructed and subjected to off-line filtering.

In the basic selection, two tracks were required with opposite charge and a distance of closest approach below 3 cm. The vertex fiducial volume was defined to be between 8 m and 33 m from the final collimator, and within 3 cm of the beam-line. Events with high hit multiplicity were rejected by requiring that no overflow condition occurred in the drift chambers. An overflow is generated if more than seven hits in a plane were recorded within 100 ns. These cuts were passed by 48.795 million events.

Events were rejected if the time difference between the tracks exceeded 6 ns. Both tracks were required to be inside the detector acceptance and within the momentum interval 10 GeV/c to 120 GeV/c. In order to allow a clear separation of pion and electron showers, we required the distance between the entry points of the two tracks at the front face of the electromagnetic calorimeter to be larger than 25 cm.

The last selection criterion was applied to a measure of the kaon momentum, to avoid the region below 50 GeV/c which is simulated inadequately. We used the sum of the moduli of the two momenta $P = P_1 + P_2$ for all decays. As a result 12.592 million events with $P > 60$ GeV/c remained. For the denominator, no identification of individual decay modes was

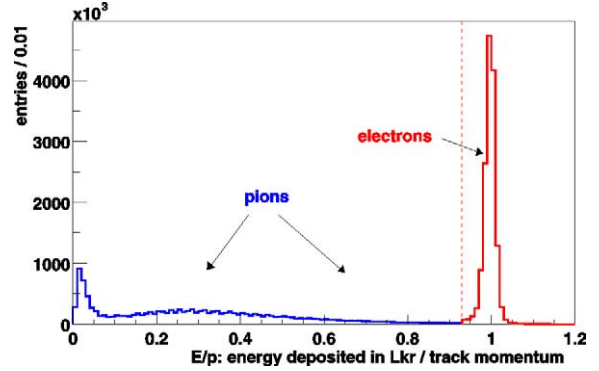


Fig. 1. The ratio of calorimetric energy E over the momentum p for the tracks of all selected K_{e3} events.

applied, and the average acceptance a_{2T} applies to the requirements listed up to this point.

For the numerator N_e , the K_{e3} signal was selected by a single additional criterion that at least one track should be consistent with an electron. This was done by requiring that the ratio E/p exceed 0.93, where E is the measured energy in the calorimeter and p is the measured momentum in the magnetic spectrometer. 6.759 million events were accepted. The quantity E/p is shown in Fig. 1 for all tracks of these K_{e3} events.

3.2. Corrections for electron identification

The number of K_{e3} events was corrected for the inefficiency of the electron identification (electrons with $E/p < 0.93$) and background coming from $K_{\mu 3}$ and $K_{3\pi}$ decays (pions with $E/p > 0.93$). Both inefficiency and background were measured from the data.

For the background determination a sample of events was selected having one track with $E/p > 1.0$, clearly classifying it as an electron. The background probability for pions $W(\pi \rightarrow e)$ was then determined from the E/p spectrum of the other (i.e., pion) track (see Fig. 2) to be

$$W(\pi \rightarrow e) = (0.576 \pm 0.005(\text{stat.}))\%.$$

As a cross check the probability was also derived from the E/p spectrum of $K_{3\pi}$ events, giving a consistent result within errors. Background from the decay $K_L \rightarrow \pi^0\pi^0\pi_D^0$ was completely removed by the cut on P .

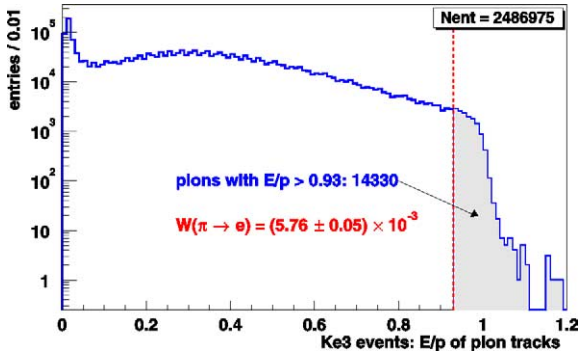


Fig. 2. Quantity E/p for pion tracks. The sample was selected by the requirement $E/p > 1.0$ for the other (i.e., electron) track.

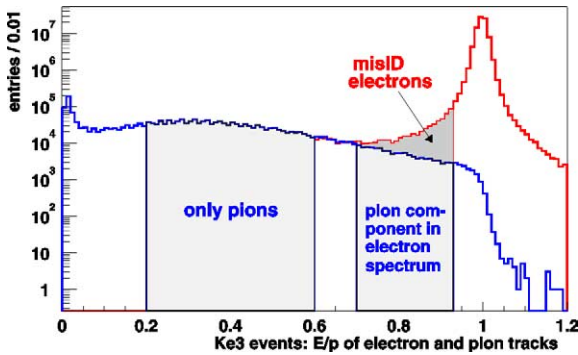


Fig. 3. Quantity E/p for electron and for pion tracks. The electron spectrum is scaled for better illustration. The dark shaded area represents electrons with $E/p < 0.93$.

The electron ID inefficiency $W(e \rightarrow \pi)$ was determined in a similar way (see Fig. 3) by requiring one track with $E/p < 0.7$, classifying it as a pion. The E/p distribution for the other track then consists mainly of electrons, with a small contribution from pions, especially below 0.7. We subtracted this pion component by using the previously determined pion distribution, normalized in the range $0.2 < E/p < 0.6$. From this we then obtained the probability for losing an electron by the condition $E/p > 0.93$:

$$W(e \rightarrow \pi) = (0.487 \pm 0.004(\text{stat.}))\%.$$

3.3. Monte Carlo simulation

To reproduce the detector response, a GEANT-based simulation of the NA48 apparatus was em-

Table 1

Detector acceptances for the charged decay modes

Decay mode	Acceptance
K_{e3}	0.2599
$K_{\mu 3}$	0.2849
$K_{3\pi}$	0.0975
$K_{2\pi}$	0.5229
$K_{3\pi_D^0}$	0.0001

ployed for the five decay modes $\pi e \nu$, $\pi \mu \nu$, $\pi^+ \pi^- \pi^0$, $\pi^+ \pi^-$ and $\pi^0 \pi^0 \pi_D^0$. Radiative corrections were included for the K_{e3} mode. We used the PHOTOS program package [4] to simulate bremsstrahlung, and added the calculations from [5] on virtual photons and electrons. Some comparisons between data and MC for identified K_{e3} events are shown in Fig. 4 (z -vertex) and Fig. 5 (x - and y -coordinates of the tracks in the first drift chamber).

We obtain the individual acceptances a_i as shown in Table 1.

The average 2-track acceptance a_{2T} was obtained from a weighted mean of the individual acceptances a_i which depends only on ratios of decay rates measured in other experiments:

$$a_{2T} = \frac{B_e a_e + B_\mu a_\mu + B_{3\pi} a_{3\pi} + B_{2\pi} a_{2\pi} + B_D a_D}{B_e + B_\mu + B_{3\pi} + B_{2\pi} + B_D} \\ = \frac{a_e \left(1 + \frac{B_\mu}{B_e} \frac{a_\mu}{a_e} + \frac{B_{3\pi}}{B_e} \frac{a_{3\pi}}{a_e} + \frac{B_{2\pi}}{B_e} \frac{a_{2\pi}}{a_e} + \frac{B_D}{B_e} \frac{a_D}{a_e} \right)}{\left(1 + \frac{B_\mu}{B_e} + \frac{B_{3\pi}}{B_e} + \frac{B_{2\pi}}{B_e} + \frac{B_D}{B_e} \right)}.$$

(6)

Here B_i are the branching ratios for the decay channels ($i = e$: K_{e3} ; $i = \mu$: $K_{\mu 3}$; $i = 3\pi$: $\pi^+ \pi^- \pi^0$; $i = 2\pi$: $\pi^+ \pi^-$; $i = D$: $\pi^0 \pi^0 \pi_D^0$). The acceptance for channel i is a_i . For the branching ratios we used a weighted average of the 2004 PDG values [1] and the new KTeV measurement [11]. The uncertainty was enlarged according to PDG rules for averaging inconsistent data.

$$B_\mu/B_e = 0.666 \pm 0.011, \quad (7)$$

$$B_{3\pi}/B_e = 0.309 \pm 0.004, \quad (8)$$

$$B_{2\pi}/B_e = (4.90 \pm 0.14) \times 10^{-3}, \quad (9)$$

$$B_D/B_e = (1.96 \pm 0.05) \times 10^{-2}. \quad (10)$$

Varying the constraints given by Eqs. (7)–(10) within their errors we get a relative variation of the acceptance of 0.16%, and $a_{2T} = 0.2412 \pm 0.0004$.

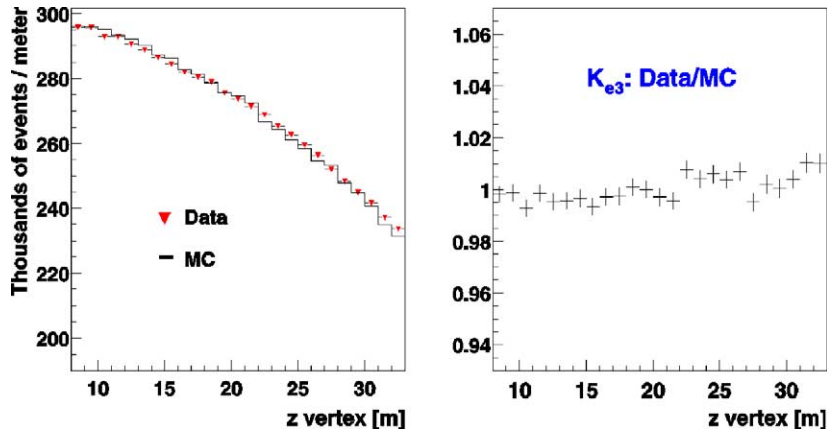


Fig. 4. Longitudinal vertex distribution for K_{e3} events: data and MC (left) and ratio of data over Monte Carlo simulation (right).

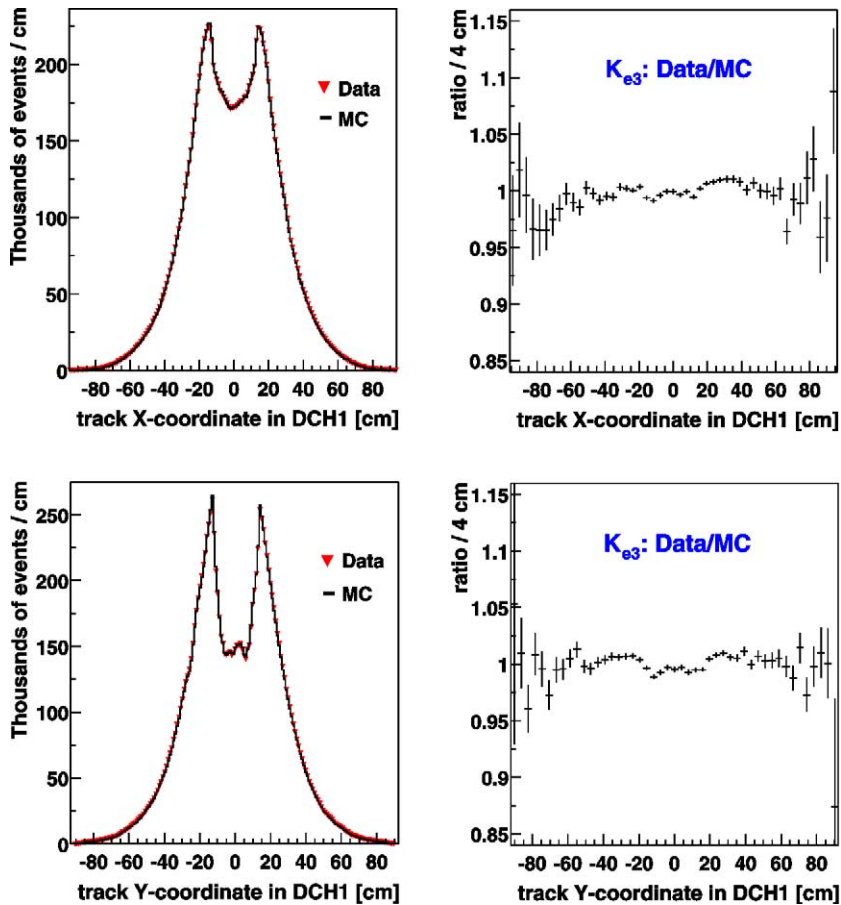


Fig. 5. Transverse positions (horizontal x and vertical y) of tracks in the first drift chamber from K_{e3} events: data and MC (left) and ratio of data over Monte Carlo simulation (right).

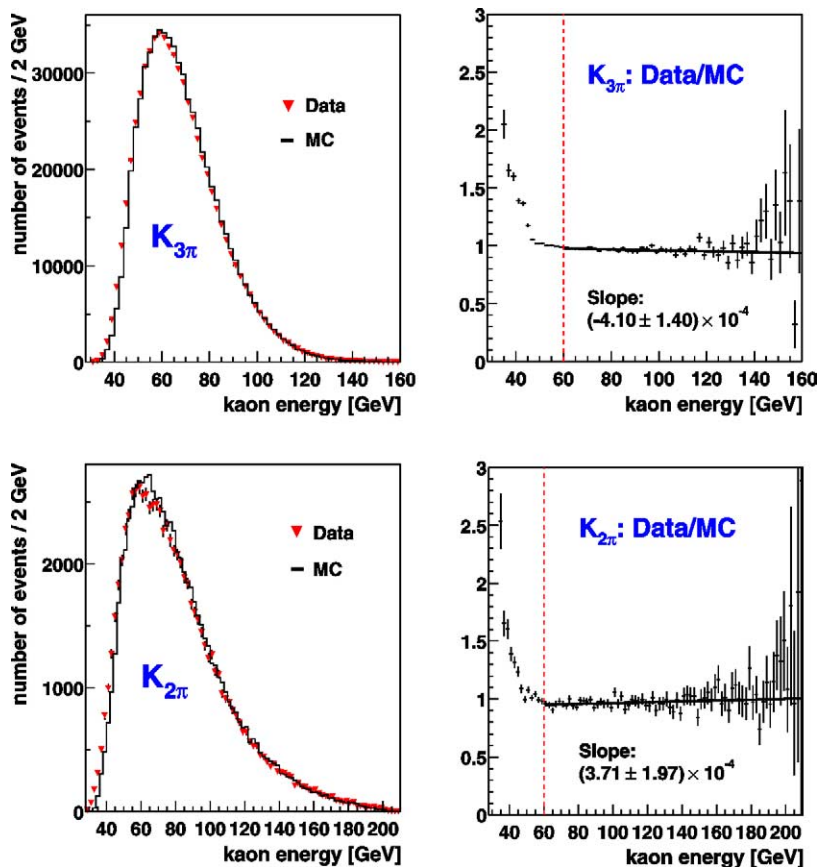


Fig. 6. Reconstructed kaon energy from $K_{3\pi}$ and $K_{2\pi}$ decays, comparison between data and MC. Errors are statistical only.

3.4. Systematic uncertainties

Given the large number of events, the uncertainties of this measurement are purely of systematic nature. Simulation shows that most of these systematics will induce a dependence of the result on the lower cut on the sum of the two moduli of the two momenta $P = P_1 + P_2$. Since the three decay modes have different neutral energy, which is either invisible as a neutrino or not used in this analysis, events with a given value of P originate from different average kaon energies, so a possible imperfection of the kaon energy spectrum (which is fairly well known for energies above 50 GeV) will induce a dependence of the result on P .

In Fig. 6 we show a comparison of the energy spectra for identified $K_{3\pi}$ and $K_{2\pi}$ events, where we can fully reconstruct the energy. Both compar-

isons show a small slope but with opposite signs, demonstrating that the kaon energy spectrum in the MC is a good compromise between different decay modes.

Fig. 7 compares the momenta of the electrons and pions in identified K_{e3} events between data and MC. Fig. 8 shows the same comparison for the sum of track momenta in the range between 60 GeV/ c and 130 GeV/ c , which contains 95% of the data. With radiative corrections applied, we still observe a slight slope in P of half the size of the slopes of the fully reconstructed events in Fig. 6. This is the dominant source of experimental uncertainty, and may be due to imperfections of the radiative corrections as well as limitations in the detailed event simulation.

To get a conservative estimate of this dependence, we varied the lower cut on the value of P from 50 GeV/ c to 80 GeV/ c . This is a large range of vari-

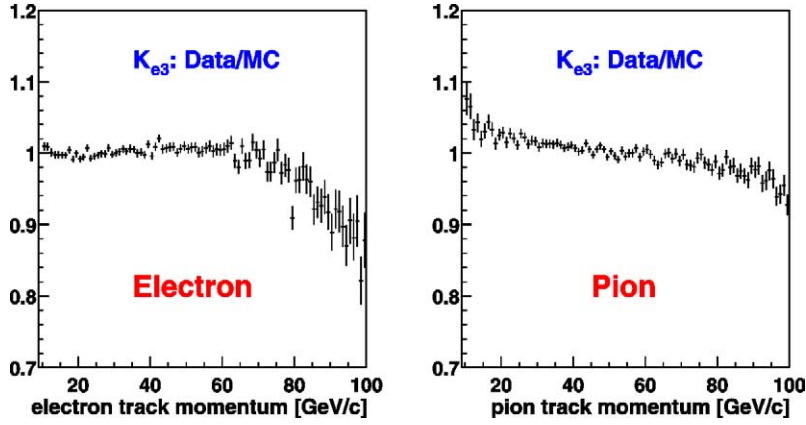


Fig. 7. Comparison between data and MC (including radiative corrections) for the momenta of electrons and pions in identified K_{e3} events. Errors are statistical only.

ation, considering that the analysis used data above 60 GeV/c, and that a cut at 80 GeV/c removes 70% of the events. The resulting relative uncertainty of the ratio R in Eq. (5) is 0.67%. In addition, a second independent analysis was performed using different selection criteria and a different kaon momentum spectrum, which was weighted such as to reproduce exactly the kaon momentum spectrum of K_{e3} events. The value of R differed from the one in the first analysis by 0.2%, well below the estimated systematic uncertainty.

To estimate the uncertainty coming from the E/p cut to select K_{e3} events, we varied the cut value between $E/p > 0.90$ and $E/p > 0.96$. As a result, inefficiency and background due to this criteria vary significantly, leading to different net corrections of K_{e3} event numbers (Table 2). Applying these corrections, however, we get almost the same number of events, thus demonstrating the correctness of this selection principle. It appears that with $E/p > 0.93$, both inefficiency and background are very small and nearly cancel. The resulting relative uncertainty on R is $\Delta R/R = 0.05\%$.

The data used in this analysis originate from two different triggers ($Q2 + (Q1/20 \cdot 2\text{trk})$, where $Q2$ requires two quadrants of the hodoscope counter to be hit, while $Q1 \cdot 2\text{trk}$ requires at least one hodoscope quadrant plus two tracks from the drift chamber trigger system. $Q1$ is prescaled by a factor of 20. By selecting one trigger, the efficiency of the other can be measured, taking into account the different downscaling. The trigger efficiencies for 2-track and K_{e3} events dif-

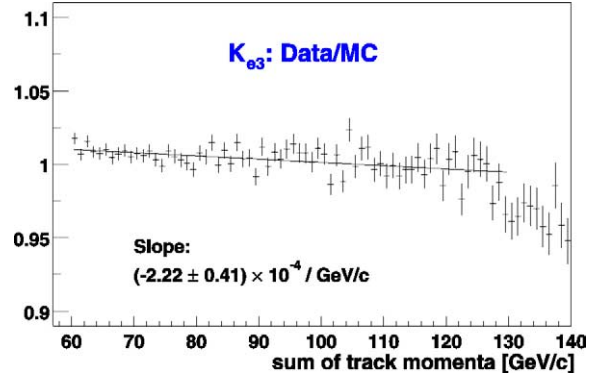


Fig. 8. Comparison between data and MC for the sum of track momenta. The region between 60 GeV/c and 130 GeV/c contains 95% of the data. Errors are statistical only.

Table 2
Variation of the E/p cut to select K_{e3} events

	$\frac{E}{p} > 0.90$	$\frac{E}{p} > 0.93$	$\frac{E}{p} > 0.96$
Inefficiency [%]	0.275	0.487	1.424
Background [%]	0.914	0.576	0.266
K_{e3} event number after E/p cut	6796461	6759184	6673114
Net K_{e3} correction	-42624	-5705	77182
Corrected K_{e3} event number	6753836	6753478	6750296

fer slightly for the $Q2$ trigger ($(97.38 \pm 0.02)\%$ for 2-track events, $(97.49 \pm 0.03)\%$ for K_{e3} events). As a check, the analysis was repeated for the $Q1 \cdot 2\text{trk}$ trigger alone, which was measured to be equally efficient

Table 3
Summary of systematic uncertainties on the ratio R

	Relative uncertainty [%]
Experimental normalization (energy spectrum)	0.67
Normalization error from input ratios	0.16
E/p cut	0.05
Trigger efficiency	0.05
DCH overflows	0.05
Magnet polarity	0.07

for all events. The relative uncertainty due to different trigger efficiencies is very small: $\Delta R/R = 0.05\%$.

In about 5% of the events the drift chambers record multiple hits in one layer which lead to an overflow condition. This could be more likely for electrons than for minimal ionizing pions or muons. Comparing the results with or without cutting on the overflow condition shows that the effect on R is almost negligible: $\Delta R/R = 0.05\%$.

Using a data set of monochromatic single pions or electrons from a test run, it has been checked that the efficiencies to record and reconstruct pions and electrons are equal within 0.05%.

In order to be independent of potential asymmetries in the setup, about half of the data were recorded with positive polarity and half with negative polarity of the spectrometer magnet. We analyzed the data separately for both polarities, but found an almost negligible difference, resulting in an uncertainty of $\Delta R/R = 0.07\%$.

As a further systematic check the analysis was repeated, broadening a number of detector resolutions in Monte Carlo. Energy, momentum and vertex positions were convoluted with Gaussian distributions, the chosen standard deviations being half of the experimental resolution. The number of selected events changed only by the order of 10^{-5} , proving that the result does not depend on resolution effects.

We summarize the systematic uncertainties on R in Table 3. Using the acceptances given in Table 1, the ratios of branching fractions from Eqs. (7)–(10) and the above evaluation of the systematic uncertainties, we obtain as average two track acceptance $a_{2T} = 0.2412 \pm 0.0004$, and a systematic uncertainty in the ratio a_e/a_{2T} of 0.68%.

4. Results

The electron identification inefficiency increases the number of K_{e3} decays by 0.49%, while background from misidentified $K_{\mu 3}$ and $K_{3\pi}$ decays reduces the number by 0.58%, leading to a net correction of -5705 events. This gives:

$$R = \frac{B(K_L \rightarrow \pi e \nu)}{B(K_L \rightarrow \text{all 2-track})} = \frac{6753478/0.2599}{12592096/0.2412} = 0.4978 \pm 0.0035. \quad (11)$$

As mentioned previously, a second independent analysis resulted in a value of R which differs by less than 0.001 from the value in Eq. (11).

For the branching ratio of the $3\pi^0$ decay, the current experimental situation is unsatisfactory. We use a weighted mean of the PDG2004 value ($21.05 \pm 0.28\%$) [1] and the recent measurement of the KTeV collaboration, ($19.45 \pm 0.18\%$) [11], and obtain ($19.92 \pm 0.70\%$), where the error is enlarged because of the poor agreement of the measurements. Therefore, the branching ratio for all 2-track events is $B(2T) = (80.56 \pm 0.70)\%$ and

$$B(e3) = \frac{\Gamma(K_L \rightarrow \pi e \nu)}{\Gamma(K_L \rightarrow \text{all})} = R \cdot B(2T) = 0.4010 \pm 0.0028 \pm 0.0035, \quad (12)$$

with the first error being the complete experimental error and the second the external error from the normalization, to be combined to

$$B(e3) = 0.4010 \pm 0.0045. \quad (13)$$

This measurement depends on three other measurements of ratios of partial K_{e3} decay widths. This dependence is given by:

$$\begin{aligned} \Delta B(e3) = & \left(\frac{\Gamma(\mu 3)}{\Gamma(e3)} - 0.666 \right) \cdot 0.077 \\ & - \left(\frac{\Gamma(3\pi)}{\Gamma(e3)} - 0.309 \right) \cdot 0.075 \\ & - \left(\frac{\Gamma(3\pi^0)}{\Gamma(e3)} - 0.515 \right) \cdot 0.151. \end{aligned} \quad (14)$$

The decay rate of $K_L \rightarrow \pi e \nu$ is obtained by using the K_L lifetime $\tau(K_L) = (5.15 \pm 0.04) \times 10^{-8}$ s [1]:

$$\Gamma(K_{e3}) = \frac{B(e3)}{\tau(K_L)} = (7.79 \pm 0.11) \times 10^6 \text{ s}^{-1}. \quad (15)$$

5. Value of $|V_{us}|$

The CKM matrix element $|V_{us}|$ can be extracted from the K_{e3}^0 decay parameters by Ref. [7]

$$|V_{us}| = \sqrt{\frac{128\pi^3 \Gamma(K_{e3}^0)}{G_F^2 M_{K^0}^5 S_{EW} I_{K^0}}} \frac{1}{f_+^{K^0\pi^-}}. \quad (16)$$

Three quantities in this equation are taken from theory. S_{EW} is the short distance enhancement factor, I_{K^0} is the phase space integral and $f_+^{K^0\pi^-}$ is the form factor.

To determine $|V_{us}|$ we follow the prescription and use the numerical results in Ref. [7], where a detailed numerical study of the K_{e3} decays to $\mathcal{O}(p^6)$ in chiral perturbation theory with virtual photons and leptons is presented. The integrals given therein correspond to the specific prescription to accept only those radiative events which have pion and electron energies within the whole K_{e3} Dalitz plot. From a Monte Carlo simulation we obtain this correction to be small

$$\frac{\text{Number of } K_{e3}(\gamma) \text{ events inside Dalitz plot}}{\text{Number of all } K_{e3}(\gamma) \text{ events}} = 0.99423. \quad (17)$$

Using Eqs. (15) and (17), $S_{EW} = 1.0232$, $I_{K^0} = 0.10339 \pm 0.00063$ we obtain a value for the product of the CKM matrix element $|V_{us}|$ and the vector form factor $f_+^{K^0\pi^-}$,

$$|V_{us}| f_+(0) = 0.2146 \pm 0.0016. \quad (18)$$

For the vector form factor, different theoretical calculations have been published recently. Chiral models including the corrections to the order p^6 give $f_+(0) = 0.981 \pm 0.010$ [7], $f_+(0) = 0.976 \pm 0.010$ [8] and $f_+(0) = 0.974 \pm 0.011$ [9], to be compared with the older value $f_+(0) = 0.961 \pm 0.010$ [6]. Lattice calculations in the quenched fermion approximation give $f_+(0) = 0.961 \pm 0.009$ [10], but this value does not include electromagnetic corrections. Taking the value from [7], which takes into account chiral corrections to the order p^6 , isospin corrections and electromagnetic corrections, we obtain the CKM element to be

$$|V_{us}| = 0.2187 \pm 0.0028. \quad (19)$$

The error on $|V_{us}|$ is dominated by the theoretical uncertainties, the error on $f_+^{K^0\pi^-}$ alone contributing ± 0.0023 .

6. Conclusions

We have made a direct measurement of the ratio of K_{e3}^0 to all K_L^0 decays with two charged tracks,

$$R = \frac{B(K_L \rightarrow \pi e \nu)}{B(K_L \rightarrow \text{all 2-track})} = 0.4978 \pm 0.0035. \quad (20)$$

Using the current experimental knowledge of the $3\pi^0$ branching ratio, this leads to a branching ratio $B(e3) = 0.4010 \pm 0.0045$. This exceeds the PDG value by $(3.3 \pm 1.3)\%$, or 2.5 standard deviations. It leads to $|V_{us}| f_+(0) = 0.2146 \pm 0.0016$, in good agreement with the recent KTeV result [11], but larger than the PDG value [1]. Inferring the most recent theoretical evaluation of $f_+(0) = 0.981 \pm 0.010$ [7], the coupling constant comes out to be $|V_{us}| = 0.2187 \pm 0.0028$, where the dominant uncertainty is theoretical. This is still 2.4 sigma lower than required by the 3-generation unitarity of the CKM matrix.

Acknowledgements

We gratefully acknowledge the continuing support of the technical staff of the participating institutes and their computing centers.

References

- [1] S. Eidelman, et al., Particle Data Group, Phys. Lett. B 592 (2004) 1.
- [2] M.A. Ademollo, R. Gatto, Phys. Rev. Lett. 13 (1964) 264.
- [3] A. Lai, et al., NA48 Collaboration, Eur. Phys. J. C 22 (2001) 231.
- [4] E. Barberio, Z. Was, Comput. Phys. Commun. 79 (1994) 291.
- [5] E.S. Ginsberg, Phys. Rev. 171 (1968) 1675;
E.S. Ginsberg, Phys. Rev. 174 (1968) 2169, Erratum;
E.S. Ginsberg, Phys. Rev. 87 (1969) 2280, Erratum.
- [6] H. Leutwyler, M. Roos, Z. Phys. C 25 (1984) 91.
- [7] V. Cirigliano, H. Neufeld, H. Pichl, Eur. Phys. J. C 35 (2004) 53.
- [8] J. Bijnens, P. Talavera, Nucl. Phys. B 669 (2003) 341.
- [9] M. Jamin, J.A. Oller, A. Pich, JHEP 0402 (2004) 047, hep-ph/0401080.
- [10] D. Becirevic, et al., hep-ph/04003217.
- [11] T. Alexopoulos, et al., hep-ex/04006002.